

Single-quantum-dot-based DNA nanosensor

CHUN-YANG ZHANG, HSIN-CHIH YEH, MARCOS T. KUROKI AND TZA-HUEI WANG*

Mechanical Engineering Department and Whitaker Biomedical Engineering Institute, The Johns Hopkins University, Baltimore, Maryland 21218, USA

*e-mail: thwang@jhu.edu

Published online: 16 October 2005; doi:10.1038/nmat1508

Rapid and highly sensitive detection of DNA is critical in diagnosing genetic diseases. Conventional approaches often rely on cumbersome, semi-quantitative amplification of target DNA to improve detection sensitivity. In addition, most DNA detection systems (microarrays, for example), regardless of their need for target amplification, require separation of unhybridized DNA strands from hybridized stands immobilized on a solid substrate, and are thereby complicated by solution–surface binding kinetics^{1,2}. Here, we report an ultrasensitive nanosensor based on fluorescence resonance energy transfer (FRET) capable of detecting low concentrations of DNA in a separation-free format. This system uses quantum dots (QDs)^{3–5} linked to DNA probes to capture DNA targets. The target strand binds to a dye-labelled reporter strand thus forming a FRET donor–acceptor ensemble. The QD also functions as a concentrator that amplifies the target signal by confining several targets in a nanoscale domain. Unbound nanosensors produce near-zero background fluorescence, but on binding to even a small amount of target DNA (~50 copies or less) they generate a very distinct FRET signal. A nanosensor-based oligonucleotide ligation assay has been demonstrated to successfully detect a point mutation⁶ typical of some ovarian tumours in clinical samples.

Several FRET-based molecular probes^{7–11} such as molecular beacons⁹ and TaqMan⁸ probes, whose fluorescence signals change as a result of hybridization or enzymatic reactions, have been developed to enable separation-free detection of DNA. FRET-based probes incorporated with single-molecule fluorescence detection technologies^{12–16} have allowed detection of unamplified, low-abundance DNA^{11,17–19}. However, accurate determination of the positive single-molecule fluorescence signals caused by FRET on hybridization has been complicated by the intrinsic background fluorescence of the probes^{17,18}, so the ultimate detection boundary and the quantitative capability of such single-molecule assays are limited.

We have developed an inorganic/organic hybrid FRET nanosensor that produces an extremely low level of background fluorescence, difficult to achieve with conventional organic FRET probes. Each DNA nanosensor consists of two target-specific oligonucleotide probes, which include a reporter probe labelled with a fluorophore and a capture probe labelled with biotin, in

addition to a QD conjugated with several streptavidins (Fig. 1a). The QD functions as both a FRET energy donor and a target concentrator. When a target DNA is present in solution, it is sandwiched by the two probes. Several sandwiched hybrids are then captured by a single QD through biotin–streptavidin binding, resulting in a local concentration of targets in a nanoscale domain. The resulting assembly brings the fluorophore acceptors and the QD donor into close proximity, leading to fluorescence emission from the acceptors by means of FRET on illumination of the donor (Fig. 1b). As a result, detection of acceptor emission indicates the presence of targets. As the unhybridized probes do not participate in FRET and are non-fluorescent, the removal of these probes becomes unnecessary. It has been demonstrated that QDs can undergo FRET phenomena and can be used to investigate interactions between proteins under ensemble measurements^{20–22}. The great photophysical properties of QDs, such as size-tunable photoluminescence spectra, broad absorption and narrow emission wavelengths and high quantum yields^{3,4,23}, make them good candidates for energy donors to overcome some of the pitfalls, such as spectral crosstalk and direct acceptor excitation, associated with conventional molecular-based FRET systems. We found that the use of single-QD-incorporated nanosensors for DNA detection can reduce significantly or even eliminate the complication of background fluorescence encountered by conventional molecular FRET probes. Further, the target signal is amplified through enhanced energy-transfer efficiency by increasing the number of acceptors linked to a donor. These features allow QD-incorporated nanosensors to generate a very distinct target signal effectively distinguishable from background in the presence of low target abundance and high probe excess.

We chose CdSe–ZnS core–shell nanocrystals, 605QD, as donors and Cy5 as acceptors (see Supplementary Information, Fig. S1, for their absorption and emission spectra). The Förster distance (R_0) for this 605QD/Cy5 FRET pair was calculated to be 69.4 Å on the basis of the Förster formalism²⁴ (see Supplementary Information, Fig. S2). Synthetic single-stranded oligonucleotides were first used to evaluate our nanosensor. A custom-made setup for confocal fluorescence spectroscopy was used to conduct fluorescence detection in which a fluorescent burst can be detected whenever a single nanosensor assembly passes through a diffraction-limited detection volume of the system (Fig. 1c).

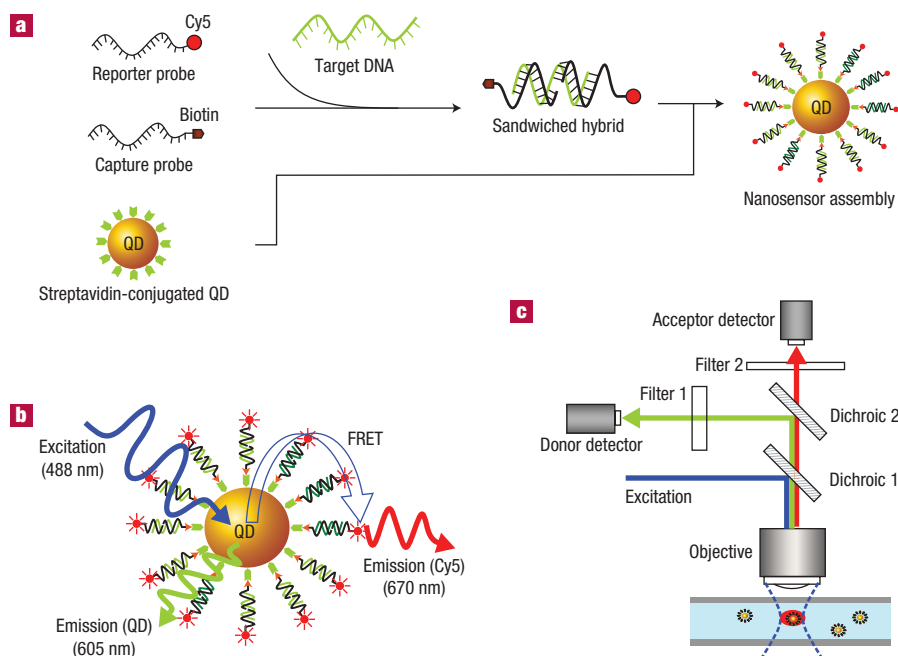


Figure 1 Schematic of single-QD-based DNA nanosensors. **a**, Conceptual scheme showing the formation of a nanosensor assembly in the presence of targets. **b**, Fluorescence emission from Cy5 on illumination on QD caused by FRET between Cy5 acceptors and a QD donor in a nanosensor assembly. **c**, Experimental setup.

To prevent photobleaching of fluorophore acceptors, we conducted the measurement in a continuous-flow manner¹⁷ inside a microcapillary such that each nanosensor assembly flowed rapidly through the laser illumination region only once. The donor and acceptor fluorescent bursts were detected by separate detectors. Figure 2a–d shows 5-s representative fluorescence signal traces detected using nanosensors. Fluorescent bursts from donors (Fig. 2a) and acceptors (Fig. 2b) were detected simultaneously when targets were present in the solution. In the absence of targets or in the presence of non-specific targets, fluorescent bursts were detected by the donor detector (Fig. 2c) but not the acceptor detector (Fig. 2d), suggesting that direct excitation of acceptors or leakage of donor emission into the acceptor detector was minimal. This near-zero background acceptor fluorescence observed in the negative control sample (Fig. 2d) also suggests high detection specificity. Energy transfer between QD donors and Cy5 acceptors was also evident in an independent experiment based on fluorescence imaging, as indicated by the Cy5 and 605QD fluorescent signals in the presence of specific targets (Fig. 2e). In contrast, only 605QD fluorescent signals were observed in the negative control experiment (Fig. 2f), indicating that energy transfer did not occur when specific targets were absent.

The selection of 605QD and Cy5 as an energy-transfer pair in the nanosensor system allows negligible crosstalk between the donor and acceptor emissions (see Supplementary Information, Fig. S1). In addition, the property of broad excitation of QDs allows sample excitation at a wavelength near the minimum of the Cy5 absorption spectrum, greatly reducing interference from direct excitation of Cy5. Although the selection of energy pairs with minimal crosstalk also leads to a decrease in the overlap between the emission spectrum of donors and the absorption spectrum of acceptors, the capability of capturing several acceptors by a QD donor helps enhance the overall energy-transfer efficiency²⁵. Therefore, highly efficient energy transfer between 605QD and Cy5 can still be achieved by increasing the number of acceptors linked

to a donor. To investigate the enhancement in energy-transfer efficiency resulting from the increase in the average acceptor/donor ratio (R) of a nanosensor assembly, we calculated the FRET factor $F = I_A / (I_A + I_D)$ at different values of R using the single-pair FRET (spFRET) analysis technique^{26,27} (Fig. 3a). I_A and I_D are the intensities of the acceptor and the donor fluorescent bursts from a single nanosensor assembly. In the negative control experiment ($R = 0$), in which fluorophore-labelled probes were not linked to QDs in the absence of specific targets, the histogram shows a peak at close to zero because fluorescent bursts were only emitted from QDs and not from Cy5. On the other hand, in measuring samples containing mixtures of nanosensors and targets, a second peak at a higher efficiency was observed owing to energy transfer from QDs to Cy5 in the presence of targets. Although only a few energy-transfer events with low energy-transfer efficiency were detected when R was 12, both the number of events and the energy-transfer efficiency were enhanced with increasing R . The histogram peaked at $F \sim 0.92$ when R was increased to 54. Further increases in R , however, did not result in higher F (data not shown), which was attributed to the depletion of the available biotin-binding sites on the streptavidin-conjugated QDs (see Methods). Similar results were obtained when measurements were made using a conventional spectrofluorimeter. Fluorescence spectra from acceptor/donor ratio (R) titration experiments showed FRET quenching of 605QD photoluminescence along with the enhancement of Cy5 photoluminescence on increasing acceptor/donor ratio (see Supplementary Information, Fig. S3). With a background fluorescence intensity and burst quantity near zero (Figs 2d,f and 3a, $R = 0$) and a high target signal intensity even in the presence of only a few targets (~ 50 or less; Fig. 2b,e), our nanosensor presents an effective method to detect low-abundance targets with high accuracy.

We characterized the change in the excited-state lifetime for donors caused by the energy-transfer process by conducting a control experiment using a 5' Cy5-labelled and 3' biotinylated oligonucleotide (see Methods). As shown in Fig. 3b, the average

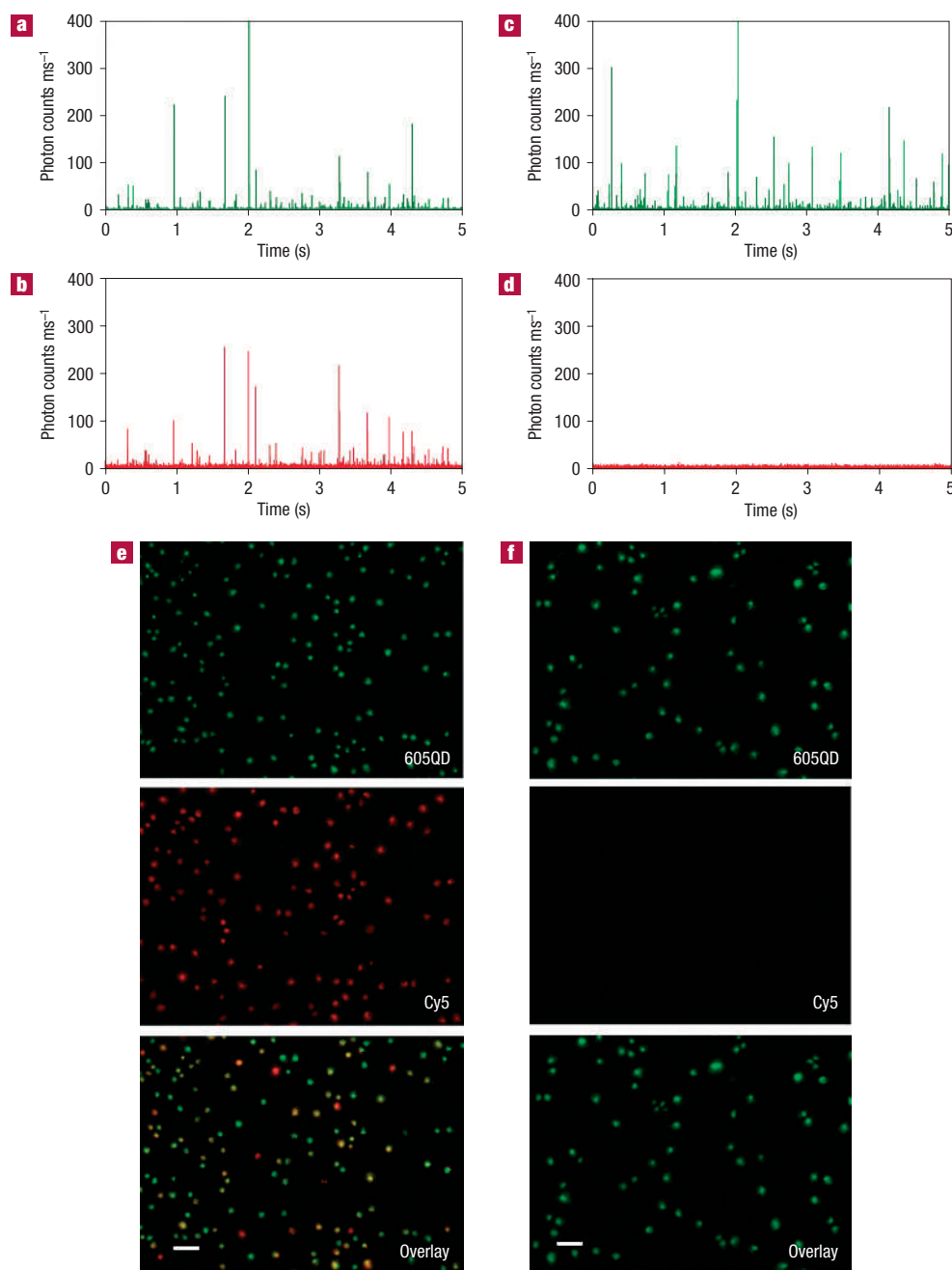


Figure 2 Detection of single-dot FRET signals. **a–d**, Representative traces of fluorescent bursts detected with nanosensors. In the presence of targets, fluorescent bursts are detected by both the donor (**a**) and the acceptor (**b**) detectors. The average intensity of acceptor fluorescent bursts was $48.3 \text{ photon counts ms}^{-1}$ against a low background of $2.1 \text{ photon counts ms}^{-1}$. When targets were absent, fluorescent bursts were only detected by the donor detector (**c**) but not by the acceptor detector (**d**). **e**, Fluorescent images of nanosensors in the presence of targets. For display purposes, fluorescent images of QDs (top) are shown in green, and images of Cy5 (middle) are shown in red. Fluorescent images with blended colours in yellow and orange (bottom) indicate co-localization of QD and Cy5. Scale bar: $10 \mu\text{m}$. **f**, Fluorescent images of nanosensors in the absence of targets. Only QD images were observed. Scale bar: $10 \mu\text{m}$. Reporter probe (Cy5-5'-GTT ACC TTG ACT AGC-3') concentration: $4.8 \times 10^{-10} \text{ M}$; capture probe (5'-TAC GAT AAG ACA GAG-3'-biotin) concentration: $4.8 \times 10^{-10} \text{ M}$; QD concentration: $2 \times 10^{-11} \text{ M}$; 30-mer DNA targets (5'-CTC TGT CTT ATC GTA GCT AGT CAA GGT AAC-3') concentration: $4.8 \times 10^{-10} \text{ M}$.

lifetime for 605QD ($\tau \sim 13.1 \text{ ns}$) decreased after it was linked with Cy5 through the oligonucleotide linkers. The lifetime further decreased to $\tau \sim 3.2 \text{ ns}$ when a 60-fold excess of Cy5-labelled linkers was added for coupling with 605QD.

To evaluate the performance of our QD-FRET-based detection platform, we compared the level of background fluorescent bursts

and the detection sensitivity of the nanosensors with molecular beacons. Molecular beacons are the most widely used hairpin energy-transfer probes for separation-free DNA hybridization detection. Owing to non-perfect energy transfer, non-perfect fluorescence quenching and conformational fluctuations of the hairpin structure under thermal agitation²⁸, unbound molecular

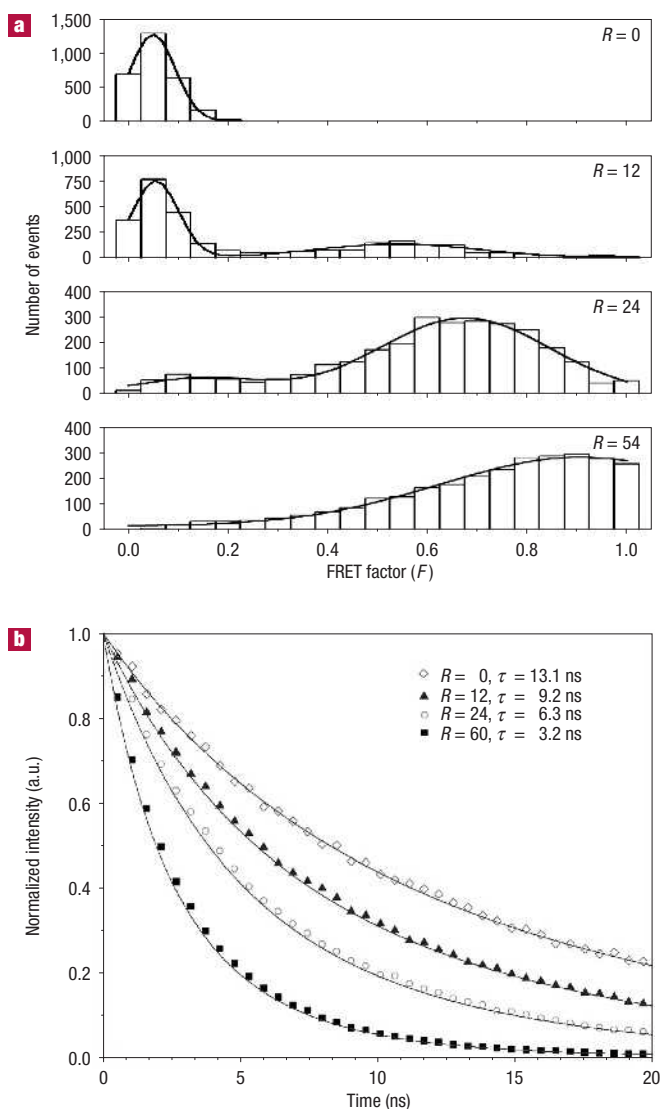


Figure 3 Characterization of FRET. **a**, FRET histograms of nanosensor assemblies at different acceptor (Cy5)/donor (QD) ratios (R). A 2×10^{-11} M solution of QDs was mixed with sandwiched hybrids of different concentrations, ranging from 0 , 2.4×10^{-10} , 4.8×10^{-10} and 10.8×10^{-10} M to prepare nanosensor assemblies with different values of R from 0 to 54 . **b**, Fluorescence lifetime decay curves and τ values at different R values. The sequence of the 5' Cy5-labelled and 3' biotinylated oligonucleotide was: Cy5-5'-CGA CCC CTG CCA CGG TCT GAG AGG TCG-3'-biotin.

beacons can produce noticeable background fluorescence^{17,18}. At any given probe concentration, the level of background fluorescent bursts from free molecular beacons was observed to be higher than that from free nanosensors (Fig. 4a). The background level of molecular beacons increased with probe concentration. In contrast, the background bursts of nanosensors remained at a minimal level (~ 0.6 fluorescent burst per 100 s or 100,000 1-ms counting events) throughout the range of probe concentrations measured. With a background level that is insensitive to increases in probe concentrations, excess probes can be added to improve the target-probe binding kinetics without an increase in background signals, making the nanosensors ideal for low-abundance target detection.

Comparison of detection sensitivity between nanosensors and molecular beacons was made on the basis of sensing responsivity,

which is defined as the ratio between the numbers of fluorescent bursts detected after and before addition of targets. As shown in Fig. 4b, the nanosensors achieved a much higher sensing responsivity than the molecular beacons at almost every target concentration tested. This result can be attributed to the excessively high intensity and quantity of fluorescent bursts generated from the nanosensor assemblies over the extremely low background. At a target concentration of 0.96 nM, the sensing responsivity of nanosensors was determined as $1,062$, which was ~ 100 -fold higher than that achieved by molecular beacons. The minimum target concentrations at which fluorescent burst signals were still distinguishable from background were 4.8 fM and 0.48 pM for nanosensors and molecular beacons, respectively.

To further validate this QD-FRET detection platform, we applied the nanosensors in combination with the oligonucleotide ligation assay (OLA)^{29,30} to the detections of Kras point mutations (codon 12 GGT to GTT mutation) in clinical samples from patients with ovarian serous borderline tumours (SBTs)⁶. Biotinylated common capture and Cy5-labelled discrimination reporter probes were designed to ligate by means of Taq DNA ligase in the presence of targets, which serve as the ligation templates (see Supplementary Information, Fig. S4). Streptavidin-functionalized QD donors were then dispatched to capture successful ligation products, facilitating energy transfer between QDs and Cy5. On the other hand, base-pair mismatch between targets and probes would prevent ligation of capture and reporter probes, and hence Cy5 acceptors and QD donors would not be brought into close proximity with each other. Consequently, perfect match and mismatch targets can be discriminated simply according to Cy5 emission. The use of nanosensors simplifies the OLA process that would otherwise require gel-separation or wash steps to remove unbound fluorescent probes²⁹⁻³¹. Figure 4c demonstrates excellent discrimination between homozygous wild-type and heterozygous targets achieved by the nanosensor-based ligation assay. The nanosensors can also be applied to other point mutation detection assays such as allele-specific primer extension (ASPE) and single-base extension (SBE) assays³¹.

In this report, we have demonstrated the extraordinary performance characteristics of a QD-FRET nanosensor for DNA detection with ultrahigh sensitivity, discrimination capacity and great simplicity. The combination of the high extinction coefficient of the dye and high QD quantum yield at a high ratio of dye acceptor per QD donor allows one to achieve efficient FRET even at a distance approaching $2R_0$. The current detection limit of our nanosensing system obviates the need for target pre-amplification and is 100-fold greater than conventional FRET probe-based assays as monitored by confocal fluorescence spectroscopy. In addition, the applications of this detection platform can be extended to other non-oligonucleotide biomolecules such as proteins and peptides by using different probe molecules in the system. Furthermore, the technology allows detection of molecular bindings in real time and at the single-molecule/particle level, and so can be applied for quantitative study of molecular interactions (for example, protein-DNA bindings and protein-ligand interactions) with high temporal and spatial resolution. Finally, the use of emission-tunable QDs as energy donors in combination with a pool of differentially labelled, target-specific probes may allow multiplex target analysis in the future and expand the detection capacity of the assay greatly.

METHODS

HYBRIDIZATION REACTION AND OLIGONUCLEOTIDE LIGATION

Hybridization reaction: The hybridization experiments were performed in a buffered solution containing 100 mM Tris-HCl, 10 mM $(\text{NH}_4)_2\text{SO}_4$, 3 mM MgCl_2 , pH 8.0. The reactions were carried out by mixing biotinylated capture probes, Cy5-labelled reporter probes and target DNA at 42°C for

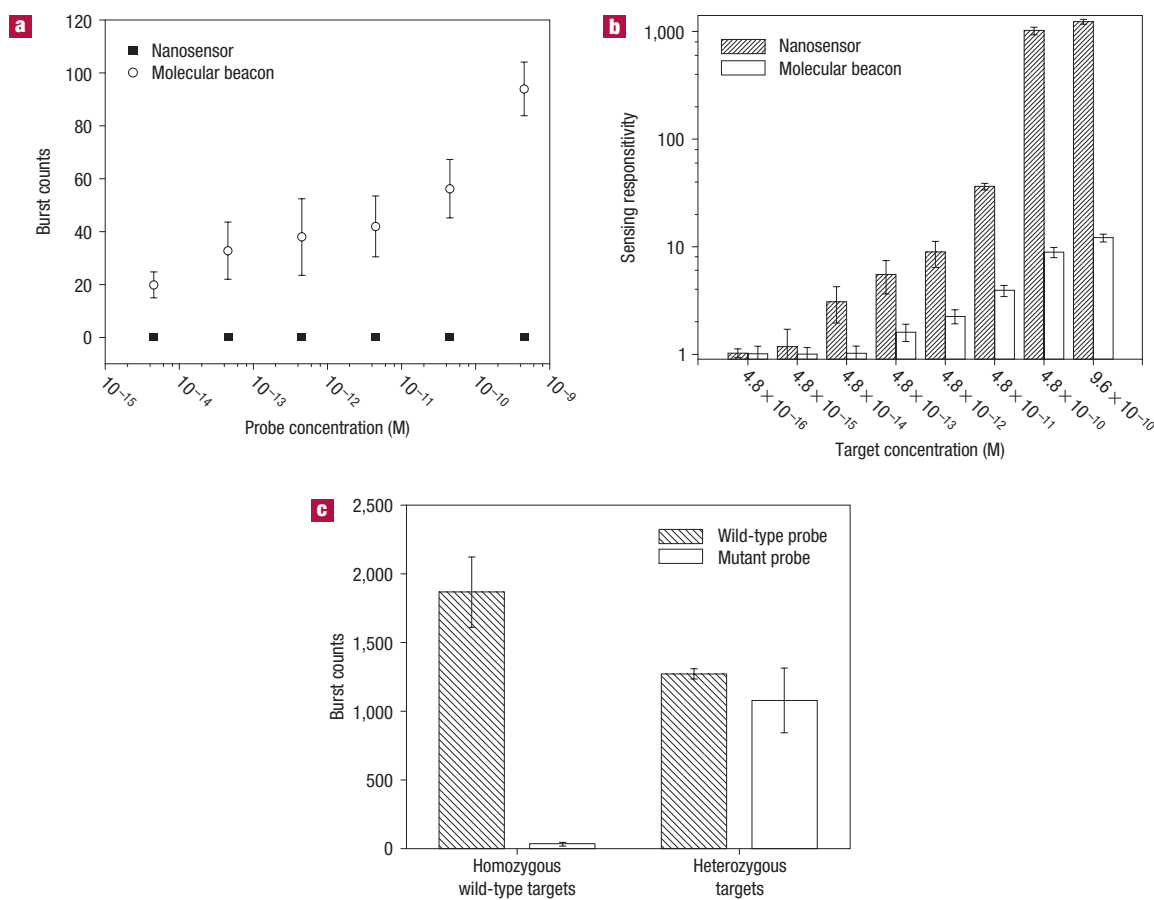


Figure 4 Evaluation of nanosensor performance. **a**, Plot of background fluorescent bursts as a function of probe concentration for QD-incorporated nanosensors and molecular beacons. For the nanosensors, the concentrations of the Cy5-labelled reporter probe and the biotinylated capture probe were kept at 1:1, and the Cy5/QD ratio was maintained at 24 in all experiments. The sequence of molecular beacons was Cy5-5'-CGACC CCTGC CACGG TCTGA GA GGTCG-3'-BHQ-2 (stems are underlined). Measurement time: 100 s. **b**, Sensing responsivity at different target concentrations for nanosensors and molecular beacons. For detection with nanosensors, the concentrations of both receptor and capture probes were kept at 4.8×10^{-10} M and the QD concentration was 2×10^{-11} M. The concentration of MB was kept at the same level as the reporter probe of nanosensors (4.8×10^{-10} M). **c**, Detection of Kras point mutations with a nanosensor-based ligation assay. Cy5-labelled discrimination reporter probes (Cy5-5'-CTC TTG CCT ACG CCA C-3' (wild-type) and Cy5-5'-CTC TTG CCT ACG CCA A-3' (mutant)) concentration: 1.2×10^{-10} M; biotinylated common capture probes (5'-CAG CTC CAA CTA CCA C-3'-biotin) concentration: 1.2×10^{-10} M; Kras homozygous wild-type targets (GGT); Kras heterozygous targets (both GGT and GTT); measurement time: 500 s. A threshold of 15 photon counts ms^{-1} was set in the Cy5 detector. Error bars show the s.d. for each experiment.

30 min (the molecular ratio of capture probes and reporter probes was kept at 1:1). After cooling to room temperature, streptavidin-functionalized QDs (Cat no. 1000-1, Quantum Dot, Hayward, California) were added to capture the sandwiched hybrids before detection. Up to ~45–75 sandwiched hybrids could be captured by a single QD as each QD was conjugated with 15–25 streptavidins (User manual: PN90-0003, Rev 5, Quantum Dot, Hayward, California), assuming three available biotin-binding sites per streptavidin after conjugation to QDs.

Oligonucleotide ligation: A 20 μl reaction mixture consisting of biotinylated common probes (0.24 pmol), Cy5-labelled discrimination probes (wild-type or mutant, 0.24 pmol), 0.5 μl PCR products (Kras homozygous wild-type or heterozygous type), two units of Taq DNA ligase and Taq ligation buffer (20 mM Tris-HCl (pH 7.6), 25 mM potassium acetate, 10 mM magnesium acetate, 10 mM dithiothreitol, 1 mM NAD^+ , 0.1% Triton X-100) was prepared for ligation reaction. Thermal cycling was performed in a MultiGene II thermal cycler (Denville, Metuchen, New Jersey) for 5 cycles using 2 min at 94°C and 4 min at 55°C . After ligation reaction, a 10 μl aliquot was removed and diluted with 89 μl PBS buffer A (10 mM sodium phosphate, 10 mM NaCl, pH 7.0). The aliquot was then heated at 85°C for 5 min to denature primer/template duplexes, followed by dipping in an ice-water bath for 5 min before detection.

EXPERIMENTAL SETUP FOR SINGLE-MOLECULE DETECTION

A custom-made setup for confocal spectroscopy was used for single-molecule detection (Fig. 1c). A 488-nm argon laser was used as an excitation light source. The laser beam was reflected by a dichroic mirror (505DCXR, Chroma Technology, Rockingham, Vermont) and focused by an oil immersion $\times 100/1.30$ NA objective lens (Olympus America, Melville, New York) to excite a sample in a 50- μm internal diameter capillary. The sample passed a laser-focused detection volume through pressure-driven flow with a syringe pump (Harvard Apparatus, Holliston, Massachusetts). The flow rate in all measurements was kept at $1 \mu\text{l min}^{-1}$. Photons emitted from the QDs and Cy5 were collected through the same objective, passed through the first dichroic mirror followed by a 50- μm pinhole (Melles Griot, Irvine, California) and then separated by another dichroic mirror (D625LP, Chroma Technology, Brattleboro, Vermont). After separation, the signal emitted from QDs was filtered by a bandpass filter (D605/20, Chroma Technology, Brattleboro, Vermont) and detected by an avalanche

photodiode (Model SPCM-AQR-13, EG&G Canada, Vaudreuil, Quebec, Canada) in the first channel (donor detector). At the same time, photons emitted from Cy5 were filtered by a bandpass filter (XF3034, Chroma Technology, Brattleboro, Vermont) and detected with another avalanche photodiode in the second channel (acceptor detector). A program written with Labview (National Instruments, Austin, Texas) and a digital counter (National Instruments, Austin, Texas) were used to perform data acquisition and data analysis. Fluorescent signals from both channels are integrated in 1-ms intervals.

QD NANOSENSOR ASSEMBLIES IMAGE ACQUISITIONS

The optical setup for fluorescence imaging consisted of an upright fluorescence microscope (Olympus America, Melville, New York), a 100-W mercury arc lamp, filter wheels for excitation filters, emission filters, dichroic mirrors and an oil immersion $\times 100/1.30$ NA objective lens. Single-molecule fluorescence images were taken by Iplab software with intensified Retiga charge-coupled-device (Qimaging, Burnaby, British Columbia, Canada). QD images were obtained with a BP 510-550 excitation filter, a BA58 IF emission filter and a 500 DRLP dichroic mirror (Omega Optical, Brattleboro, Vermont). The Cy5 images were obtained with a 475AF40 excitation filter, a 670DF40 emission filter and a 595DLPBX-04 dichroic mirror (Omega Optical, Brattleboro, Vermont).

Received 9 May 2005; accepted 1 September 2005; published 16 October 2005.

References

- Southern, E., Mir, K. & Shchepinov, M. Molecular interactions on microarrays. *Nature Genet.* **21**, 5–9 (1999).
- Taton, T. A., Mirkin, C. A. & Letsinger, R. L. Scanometric DNA array detection with nanoparticle probes. *Science* **289**, 1757–1760 (2000).
- Chan, W. C. W. & Nie, S. M. Quantum dot bioconjugates for ultrasensitive nonisotopic detection. *Science* **281**, 2016–2018 (1998).
- Bruchez, M., Moronne, M., Gin, P., Weiss, S. & Alivisatos, A. P. Semiconductor nanocrystals as fluorescent biological labels. *Science* **281**, 2013–2016 (1998).

5. Medintz, I. L., Uyeda, H. T., Goldman, E. R. & Mattoussi, H. Quantum dot bioconjugates for imaging, labelling and sensing. *Nature Mater.* **4**, 435–446 (2005).
6. Ho, C. L., Karman, R. J., Dehari, R., Wang, T. L. & Shih, I. M. Mutations of BRAF and KRAS precede the development of ovarian serous borderline tumors. *Cancer Res.* **64**, 6915–6918 (2004).
7. Cardullo, R. A., Agrawal, S., Flores, C., Zamecnik, P. C. & Wolf, D. E. Detection of nucleic-acid hybridization by nonradiative fluorescence resonance energy-transfer. *Proc. Natl Acad. Sci. USA* **85**, 8790–8794 (1988).
8. Holland, P. M., Abramson, R. D., Watson, R. & Gelfand, D. H. Detection of specific polymerase chain-reaction product by utilizing the 5' → 3' exonuclease activity of thermus-aquaticus dna-polymerase. *Proc. Natl Acad. Sci. USA* **88**, 7276–7280 (1991).
9. Tyagi, S. & Kramer, F. R. Molecular beacons: Probes that fluoresce upon hybridization. *Nature Biotechnol.* **14**, 303–308 (1996).
10. Dubertret, B., Calame, M. & Libchaber, A. J. Single-mismatch detection using gold-quenched fluorescent oligonucleotides. *Nature Biotechnol.* **19**, 365–370 (2001).
11. Knemeyer, J. P., Marmé, N. & Sauer, M. Probes for detection of specific DNA sequences at the single-molecule level. *Anal. Chem.* **72**, 3717–3724 (2000).
12. Barnes, M. D., Ng, K. C., Whitten, W. B. & Ramsey, J. M. Detection of single rhodamine-6g molecules in levitated microdroplets. *Anal. Chem.* **65**, 2360–2365 (1993).
13. Shera, E. B., Seitzinger, N. K., Davis, L. M., Keller, R. A. & Soper, S. A. Detection of single fluorescent molecules. *Chem. Phys. Lett.* **174**, 553–557 (1990).
14. Nie, S. M., Chiu, D. T. & Zare, R. N. Probing individual molecules with confocal fluorescence microscopy. *Science* **266**, 1018–1021 (1994).
15. Eigen, M. & Rigler, R. Sorting single molecules—application to diagnostics and evolutionary biotechnology. *Proc. Natl Acad. Sci. USA* **91**, 5740–5747 (1994).
16. Castro, A. & Williams, J. G. K. Single-molecule detection of specific nucleic acid sequences in unamplified genomic DNA. *Anal. Chem.* **69**, 3915–3920 (1997).
17. Wang, T. H., Peng, Y. H., Zhang, C. Y., Wong, P. K. & Ho, C. M. Single-molecule tracing on a fluidic microchip for quantitative detection of low-abundance nucleic acids. *J. Am. Chem. Soc.* **127**, 5354–5359 (2005).
18. Zhang, C. Y., Chao, S. Y. & Wang, T. H. Comparative quantification of nucleic acids using single-molecule detection and molecular beacons. *Analyst* **130**, 483–488 (2005).
19. Wabuyele, M. B. *et al.* Approaching real-time molecular diagnostics: Single-pair fluorescence resonance energy transfer (spFRET) detection for the analysis of low abundant point mutations in K-ras oncogenes. *J. Am. Chem. Soc.* **125**, 6937–6945 (2003).
20. Medintz, I. L. *et al.* A fluorescence resonance energy transfer-derived structure of a quantum dot-protein bioconjugate nanoassembly. *Proc. Natl Acad. Sci. USA* **101**, 9612–9617 (2004).
21. Medintz, I. L. *et al.* Self-assembled nanoscale biosensors based on quantum dot FRET donors. *Nature Mater.* **2**, 630–638 (2003).
22. Willard, D. M., Carillo, L. L., Jung, J. & Van Orden, A. CdSe-ZnS quantum dots as resonance energy transfer donors in a model protein-protein binding assay. *Nano Lett.* **1**, 469–474 (2001).
23. Mattoussi, H. *et al.* Self-assembly of CdSe-ZnS quantum dot bioconjugates using an engineered recombinant protein. *J. Am. Chem. Soc.* **122**, 12142–12150 (2000).
24. Clapp, A. R. *et al.* Fluorescence resonance energy transfer between quantum dot donors and dye-labeled protein acceptors. *J. Am. Chem. Soc.* **126**, 301–310 (2004).
25. Lakowicz, J. R. *Principles of Fluorescence Spectroscopy* (Kluwer Academic/Plenum, New York, 1999).
26. Ha, T. *et al.* Ligand-induced conformational changes observed in single RNA molecules. *Proc. Natl Acad. Sci. USA* **96**, 9077–9082 (1999).
27. Deniz, A. A. *et al.* Single-pair fluorescence resonance energy transfer on freely diffusing molecules: Observation of Forster distance dependence and subpopulations. *Proc. Natl Acad. Sci. USA* **96**, 3670–3675 (1999).
28. Bonnet, G., Krichevsky, O. & Libchaber, A. Kinetics of conformational fluctuations in DNA hairpin-loops. *Proc. Natl Acad. Sci. USA* **95**, 8602–8606 (1998).
29. Landegren, U., Kaiser, R., Sanders, J. & Hood, L. A ligase-mediated gene detection technique. *Science* **241**, 1077–1080 (1988).
30. Nickerson, D. A. *et al.* Automated DNA diagnostics using an elisa-based oligonucleotide ligation assay. *Proc. Natl Acad. Sci. USA* **87**, 8923–8927 (1990).
31. Kwok, P. Y. *Single Nucleotide Polymorphisms Methods and Protocols* (Human Press, Totowa, New Jersey, 2003).

Acknowledgements

The authors thank Y. Peng, S. Yang, S. Lin and Y. P. Ho for valuable discussions, I. M. Shih for providing us with PCR products from clinical samples for Kras point mutation detections, and L. Brand and D. Toptygin for providing support with the TCSPC fluorescence lifetime measurements. This work was supported primarily by NSF under award no. DBI-0352407 and also by the Whitaker Foundation.

Correspondence and requests for materials should be addressed to T.-H.W. Supplementary Information accompanies this paper on www.nature.com/naturematerials.

Competing financial interests

The authors declare that they have no competing financial interests.

Reprints and permission information is available online at <http://npg.nature.com/reprintsandpermissions/>